Journal of Chromatography B 1231 (2023) 123937

Contents lists available at ScienceDirect

Journal of Chromatography B

journal homepage: www.elsevier.com/locate/jchromb

Detection of tuberculosis-associated compounds from human skin by GCxGC-TOFMS

Portia C.K. Makhubela [a], Egmont R. Rohwer [a], Yvette Naudé [a,*]

[a] Department of Chemistry, University of Pretoria, Private Bag X20, Hatfield, 0028 Pretoria, South Africa

ARTICLE INFO

Keywords:
Human skin volatiles
Non-invasive wearable sampler
GCxGC-TOFMS
Predictive modelling
Tuberculosis biomarkers

ABSTRACT

Tuberculosis (TB) remains a global health concern. This study aimed to investigate the potential of human skin volatile organic compounds (VOCs) as prospective biomarkers for TB diagnosis. It employed a non-invasive approach using a wearable silicone rubber band for VOC sampling, comprehensive gas chromatography – time of flight mass spectrometry (GCxGC-TOFMS), and chemometric techniques. Both targeted and untargeted biochemical screening was utilized to explore biochemical differences between healthy individuals and those with TB infection. Results confirmed a correlation between compounds found in this study, and those reported for TB from other biofluids. In a comparison to known TB-associated compounds from other biofluids our analysis established the presence of 27 of these compounds emanating from human skin. Additionally, 16 previously unreported compounds were found as potential biomarkers. The diagnostic ability of the VOCs selected by statistical methods was investigated using predictive modelling techniques. Artificial neural network multilayered perceptron (ANN) yielded two compounds, 1H-indene, 2,3 dihydro-1,1,3-trimethyl-3-phenyl; and heptane-3-ethyl-2-methyl, as the most discriminatory, and could differentiate between TB-positive (n = 15) and TB-negative (n = 23) individuals with an area under the receiver operating characteristic curve (AUROC) of 92 %, a sensitivity of 100 % and a specificity of 94 % for six targeted features. For untargeted analysis, ANN assigned 3-methylhexane as the most discriminatory between TB-positive and TB- negative individuals. An AUROC of 98.5 %, a sensitivity of 83 %, and a specificity of 88 % were obtained for 16 untargeted features as chosen by high performance variable selection. The obtained values compare highly favourable to alternative diagnostic methods such as breath analysis and GeneXpert. Consequently, human skin VOCs hold considerable potential as a TB diagnostic screening test.

1. Introduction

Tuberculosis (TB) is a contagious, airborne bacterial infection caused by *Mycobacterium tuberculosis* (*M.tb*) [1]. The most common form of infection in humans is pulmonary TB; it affects the lungs and occurs in over 80 % of TB cases [2]. It is one of the leading causes of death in low- and middle-income countries. Despite medical and technological advances, blood and sputum samples are still the only primary biological materials used in the detection of TB by various diagnostic tests. Current TB diagnostic tests all require a good quality sputum sample, which is not always possible for individuals to produce when presenting with a dry cough [3,4]. Individuals that cannot produce an adequate sputum sample are subjected to more invasive methods, such as gastric aspirate which increases the costs of an already expensive TB test [5,6]. This highlights the need for alternative, non-invasive biological sampling materials in TB diagnosis.

Advances in separation sciences have seen an increase in diagnostic biomarker discovery research, with a focus on proteomics, metabolomics, and the human volatilome [7–14]. A number of research groups investigated TB diagnostic test methods capable of providing results in a short period, or using alternative biological sampling materials, instead of the conventional blood or sputum samples [12–16]. Test methods include hyphenated chromatographic methods involving alternative matrices such as urine and breath [7,12–15,17,18]. These alternative matrices are based on the premise that VOCs excreted from the body are related to the metabolic state of the individual, and therefore indicative of physiological processes [19]. Studies that have investigated VOCs in breath, sputum and cultured samples during active pulmonary TB to identify compounds associated with TB each reported different compound markers [7,11–14], of which a selection is given in Table 1.

* Corresponding author.
E-mail address: yvette.naude@up.ac.za (Y. Naudé).

https://doi.org/10.1016/j.jchromb.2023.123937
Received 7 July 2023; Received in revised form 28 September 2023; Accepted 10 October 2023
Available online 18 November 2023

Table 1
Twenty-seven VOC TB biomarkers detected from TB-positive participant skin emanations.

Class	Compound from skin	TB-associated compound (literature)	Molecular weight	Molecular formula	Cas Number	Fisher's exact test (*p*-value)	Retention Indices ^{1}D experimental	Retention Indices Literature (non-polar)	Normalised peak area Decreased (↓) or increased (↑) in TB-positive group
Alkanes	Pentane-2,3-dimethyl	Breath [13]	100	C7H16	565–59-3	1	<800	659	
	Cyclohexane-1-ethyl-4-methyl	Breath [13]	126	C9H18	6236–88-0	0.478	887	888	
	Heptane-2,4-dimethyl	Breath [13]	128	C9H20	2213–23-2	0.524	810	816	
	Heptane-5-ethyl-2-methyl	Breath [32]	142	C10H22	13475–78-0	0.675	928	925	
	Octane-2,6-dimethyl	Breath [13]	142	C10H22	2051–30-1	0.483	933	934	
	Heptane-3-ethyl-2-methyl *	Breath [13]	142	C10H22	14676–29-0	0.002	941	942	↑
	Decane-4-methyl	Breath [13]	156	C11H24	2847–72-5	0.224	1064	1062	
	Cyclohexane-hexyl	Breath [32]	168	C12H24	4292–75-5	0.085	1253	1259	
	Decane-3,7-dimethyl	Breath [32]	170	C12H26	17312–54-8	0.047	1130	1133	
	Dodecane #	Breath, *M.tb* culture, sputum [14]	170	C12H26	112–40-3	Present in every participant	1202	1200	
	Tridecane	Breath [13,32]	184	C13H28	629–50-5	0.395	1309	1300	
Alkenes	1-Hexene-4-methyl	Breath [32]	98	C7H14	3769–23-1	0.645	<800	665	
	1-Octene*	Breath [13]	112	C8H16	111–66-0	0.013	<800	782	↑
	1-Nonene-4,6,8-trimethyl	Breath [32]	168	C12H24	54410–98-9	0.104	1010	1012	
Alcohols	Benzenemethanol,α,α,-dimethyl	Breath [13]	136	C9H12O	617–94-7	1	1052	1057	
	1-Octanol-2-butyl	Breath [13]	186	C12H26O	3913–02-8	0.636	1274	1277	
Aldehydes	Acetaldehyde*	Breath [13]	44	C2H4O	75–07-0	0.007	<800	381	↓
	Heptanal*,#	Breath [13]	114	C7H14O	111–71-7	0.024	879	882	↓
	Octanal*,#	Breath [14]	128	C8H16O	124–13-0	0.036	985	982	↓
	Nonanal #	Breath [13]	142	C9H18O	124–19-6	1	1083	1081	
Ketones	2-Butanone	Breath [13]	72	C4H8O	78–93-3	0.061	<800	581	
	Cyclohexanone	*M.tb* culture [14]	98	C6H10O	108–94-1	0.302	853	852	
Carboxylic acid	Tetradecanoic acid	Breath [14]	228	C14H28O2	544–63-8	0.395	1746	1748	
Aromatics	Styrene	Breath [13]	104	C8H8	100–42-5	0.061	912	914	
	o-Xylene	Urine [30]	106	C8H10	95–47-6	0.478	866	862	
	Naphthalene-1-methyl	Breath [13]	142	C11H10	90–12-0	0.085	1291	1289	
	1H-Indene − 2,3-dihydro-1,1,3-trimethyl-3-phenyl*	Breath [13]	236	C18H20	3910–35-8	0.001	1719	1716	↓

<800: Retention Index standard C_8-C_{28}.
Literature Retention Indices from NIST 14 library.
M.tb = *mycobacteria tuberculosis*.
* Compounds retained at a 95 % confidence level as being significantly different between patient and control groups (p-values ≤ 0.05).
# Confirmed with analytical standards.

A comparative study of breath VOCs *versus* skin VOCs following ingestion of glucose by Turner *et al.* (2004) reported that most VOCs detected in breath were also present in the skin albeit at a lower concentration, therefore, there is a correlation between skin emanations and exhaled breath [20]. Sampling of human skin emanations is appealing, since breath is considered a more infectious matrix in a TB context, and moreover requires trained medical staff for sample collection. Sampling methods for VOCs from skin include glass beads, nylon socks, PTFE (Teflon™) sleeves and cellulose bags, with the most frequently used sorbents in collection traps ranging from carbon molecular sieves to different types of graphite and organic polymers [21,22]. Disadvantages are long sampler deployment periods and bulky samplers which require additional non-wearable equipment. To overcome these limitations Roodt *et al.* (2018) developed a skin sampling method using an in-house made polydimethylsiloxane (PDMS) silicone rubber band sampler [23]. Roodt's study demonstrated the ability of PDMS to adequately sample skin emanations with ease due to the small size of the rubber bands and a shorter sampling period [23]. This skin sampling technique was then improved by Wooding et al. (2020) by incorporation of an aluminized Mylar® covering as a barrier to prevent background contamination during skin emanations sampling [24,25]. Following a similar approach Vishinkin et al. (2021) sampled skin headspace onto a poly(2,6-diphenylphenylene oxide) pouch, which yielded four TB-specific VOCs (acetic acid, 2-ethyl-1-hexanol, hexyl butyrate, and toluene) after thermal desorption-GC–MS [22].

We report skin VOCs from TB-positive participants and TB-negative controls collected with a silicone rubber band (PDMS) sampler followed by thermal desorption – comprehensive gas chromatography – time of flight mass spectrometry (TD-GCxGC-TOFMS). Multivariate analysis of the data was two-fold: 1) a targeted approach where compounds found in this study were compared to known TB-associated compounds from other biofluids; and 2) an untargeted approach with an emphasis on exploring compounds previously unreported in the literature that may serve as TB biomarkers.

2. Material and methods

2.1. Ethical considerations

This study was approved by the ethics committees of the Faculty of

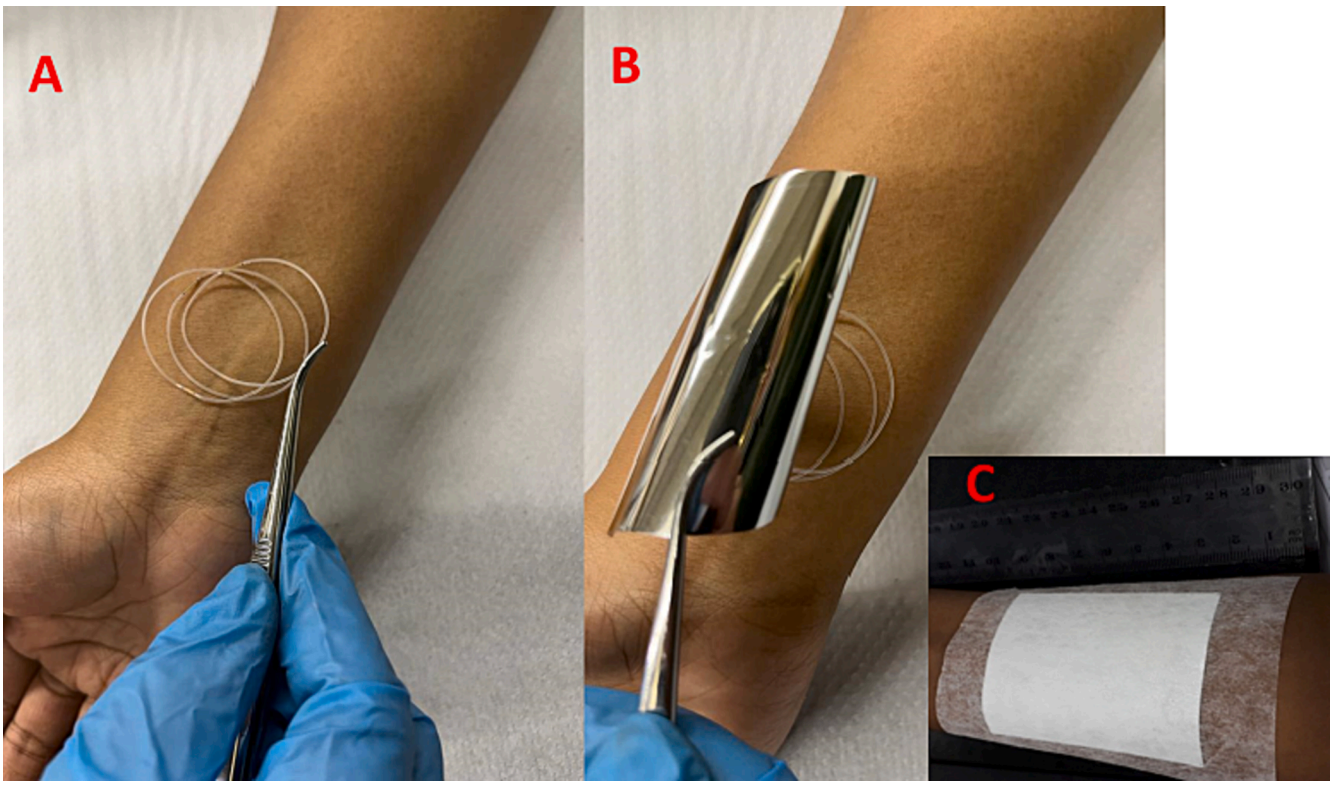

Fig. 1. Skin VOCs sampling. (A) positioning of the three ethanol-modified silicone rubber band samplers on the inner arm, (B) Mylar® cover, (C) hypoallergenic Micropore™ paper tape covering.

Health Sciences and the Faculty of Natural and Agricultural Sciences (references: 300/2018 and EC180306-176) of the University of Pretoria. Permission to conduct the study in its hospitals were obtained from Steve Biko Academic Hospital and the Tshwane District Hospital, Pretoria, South Africa.

Prior written consent was obtained from the participants.

2.2. Study cohort

The pilot study cohort consisted of test and control groups, both containing male and female participants (n = 38) (Table S1). Each participant was sampled in triplicate, and analysed in duplicate. Fifteen patients were clinically diagnosed with TB. These participants were sampled (2018) before commencement with TB drug treatment. The treatment naive control group (n = 23) was confirmed to be TB-negative. TB-positive status was confirmed by GeneXpert MTB/RIF assay (Cepheid, Sunnyvale, CA, USA) and TB- negative status was confirmed by QuantiFeron-TB gold assay (Cellestis/Qiagen, Carnegie, Australia) coupled with Fourth generation HIV-1/2 ELISA assay (Abbott diagnostics medical co. Ltd, Lake Forest, IL, USA) to rule out false-positive results. Participant demographic information is provided in Table S1. Participants from group one (clinically TB-positive) were sampled at the Steve Biko Academic Hospital and the Tshwane District Hospital, Pretoria, South Africa. Participants from group two (clinically TB-negative) were all either students, or staff, of the University of Pretoria (UP) and samples were collected on the premises of the UP in 2018. Participants were required to complete a questionnaire to disclose, inter alia, diet, smoking, exercise routine, and the use of medication and personal care products over the last 24 h prior to sampling to account for potential variations in VOC profiles resulting from these factors (Table S2).

2.3. Analytical standards

The solution of *n*-alkanes (C_8-C_{28}) used for the calculation of linear retention indices of reported analytes was purchased from Merck, Pretoria, South Africa. Analytical standards of heptanal (≥95 %), octanal (≥95 %), and nonanal (≥99.5 %) were purchased from Sigma-Aldrich (Pty) Ltd., Kempton Park, South Africa, and were used for confirming the presence of these target analytes.

2.4. Skin sampling

Wearable, laboratory-constructed polydimethylsiloxane (PDMS) (silicone rubber) sampling bands were prepared by cutting ten cm lengths of medical grade silicone elastomer tubing (0.64 mm OD x 0.3 mm ID, Sil-Tec Technical Products, Georgia, USA) which were joined end-to-end with a 1 cm length of uncoated capillary column (0.25 mm ID; SGE Analytical Science, Separation Scientific (Pty), Roodepoort, South Africa) [23–26]. Each band had a PDMS mass of 30–35 mg.

Before use the PDMS bands were cleaned and conditioned according to a method by Triñanes et al. (2005) [27]. To improve the sampling efficiency of polar compounds, and to increase the total sorption volume, the PDMS samplers were solvent-modified as follows: one end of a PDMS band was opened by removing the uncoated capillary coupling, the sampler was then placed in a glass vial containing ethanol (Sigma-Aldrich®, South Africa) followed by five minutes of ultra-sonication. The solvent impregnated sampler was removed from the solvent and fashioned back into a loop configuration by re-inserting the uncoated capillary coupling. The PDMS loop was then suspended above approximately one mL of ethanol in a glass vial to create a saturated environment to prevent the evaporation of the polar solvent inside the PDMS band sampler.

Each participant was sampled by placing three sampling bands on the skin. GCxGC-TOFMS analyses were done on two of the set of three sampling bands, with the remaining band kept as a back-up. The skin

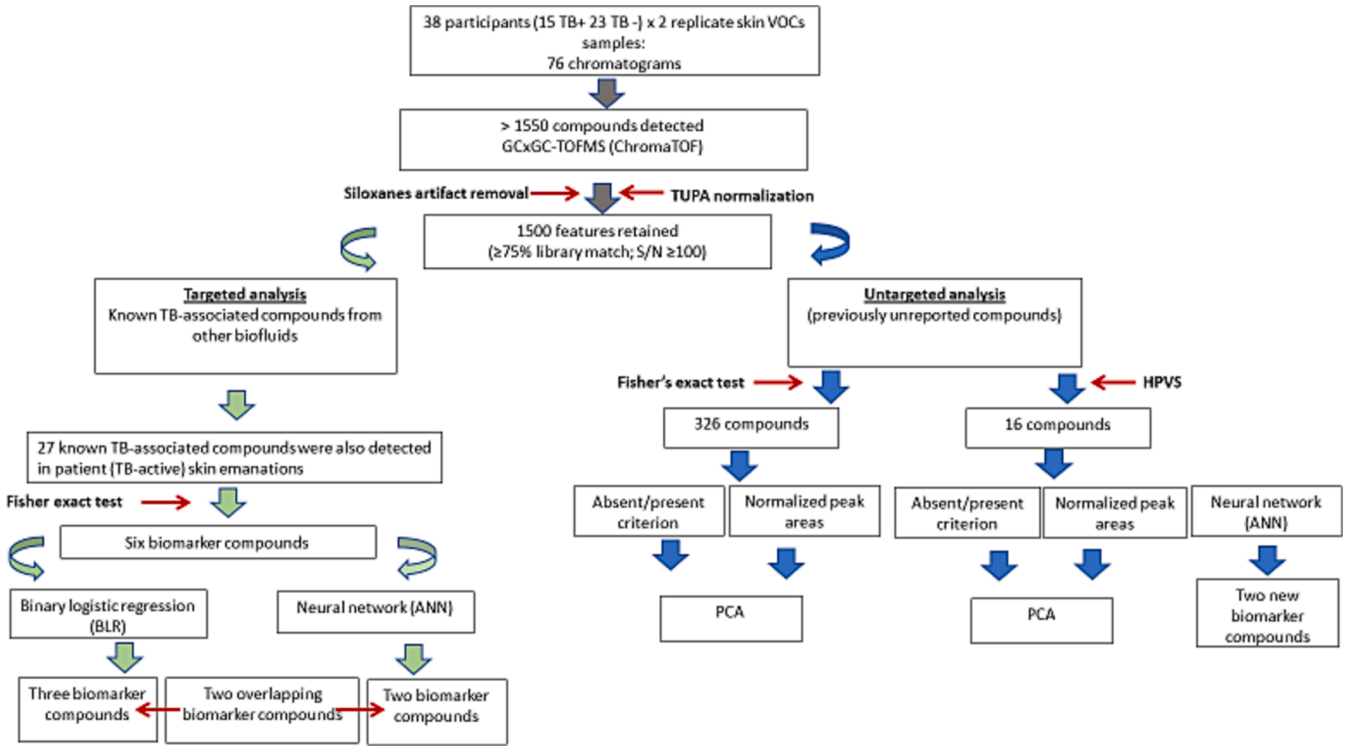

Fig. 2. Schematic diagram of the data processing workflow.

sampling area (inner arm) was cleaned with 70 % v/v isopropanol pads (Medic + dressings, Dischem, Hillcrest, South Africa). Three PDMS bands modified with ethanol were placed on the cleaned patch of inner arm skin, covered with aluminized Mylar® sheeting (10 cm × 6 cm; Hydroponic, South Africa) and attached to the skin with hypoallergenic 3 M Micropore™ adhesive surgical paper tape (12 cm L x 7.2 cm W, Dischem, Hillcrest, South Africa) (Fig. 1).

The Mylar® barrier served to exclude exogenous compounds from the environment during skin emanation sampling. [24,25].

The sampling patch ensemble was worn for an hour during which the participants were free to continue with their daily routine. After a one hour sampling period the patch was removed and the silicone rubber bands were returned to the ethanol saturated glass vial. A piece of heavy-duty aluminium foil with the shiny side facing the cap (16 µm, heavy-duty foil, Pick 'n Pay, South Africa) was placed between the glass vial and the Teflon coated lid before capping the vial, to prevent absorptive competition between the PDMS bands and the Teflon coated cap. The vial was then covered in foil to protect the sample from light, it was kept cool during transport to the laboratory and stored in a freezer at −18 °C prior to analysis.

2.5. Analysis by TDS-GCxGC-TOFMS

Analyses were done in duplicate, i.e. two PDMS sampling bands from each set of three were analysed. Blanks (empty desorption tubes) were analysed between each set of sampling bands, in addition to laboratory blanks (blank sampling bands). Instrumental analysis was performed on a LECO Pegasus 4D GC × GC-TOFMS fitted with a Gerstel TDS unit as an inlet, an Agilent 7890 gas chromatograph and a dual quad-jet cryogenic modulator (LECO, Kempton Park, South Africa), operated by ChromaTOF software (version 4.50.8.0). The hot jets were operated with synthetic air and the cold jets were operated with nitrogen gas (NM3OLA ML nitrogen gas generator, Peak Scientific, South Africa) cooled with liquid nitrogen (Afrox, South Africa). The primary (1D) capillary column was a Rxi-1MS of length 30 m, 0.25 mm ID and 0.25 µm film thickness; the secondary (2D) column was a Rxi-17SilMS mid-polar capillary column of length 0.760 m, 0.25 mm ID and 0.25 µm film thickness.

Thermal desorption of the compounds from the PDMS sampling bands was performed using a Gerstel™ thermal desorption unit (TDS 3, Chemetrix, Midrand, South Africa), with the bands inserted into a glass thermal desorption tube. Desorption was from 30℃ (held for 3 min) to 250℃ (held for 10 min) at 60℃/min, with a flow rate of 100 mL/min helium (ultra-high purity grade; Afrox, Gauteng, South Africa). The TDS transfer line temperature was maintained at 350℃. Cryogenic focussing of the desorbed compounds occurred at −100℃, using liquid nitrogen (Afrox, Gauteng, South Africa) in a cooled injection system (Gerstel™ CIS 4) with an empty, baffled and deactivated glass liner. The thermally desorbed compounds were introduced into the inlet *via* a splitless injection (purge flow of 30 mL/min after 90 s, solvent vent mode) by heating the CIS from −100℃, at 10℃/s, to 250℃ (held for the duration of the GC run). The helium carrier gas Africa]) flow-rate was constant at 1.4 mL/min.

The primary oven temperature programme was 40℃ for 1.5 min, and ramped to 280℃ at a rate of 10℃/min, with a hold time at this temperature of 3 min. The total run time was 28.5 min. The temperature programme rates for the secondary oven and the modulator were the same as that of the primary oven, but offset by + 5℃ and + 15℃ respectively. The modulation period was 3 s with a hot pulse time of 0.8 s. The transfer line to the TOFMS was maintained at a temperature of 280℃. The acquisition rate was 100 spectra/second over a mass range of 35–500 Daltons. The ionisation energy was 70 eV in the electron impact ionisation mode (EI +), the voltage of the detector was 1750 V, and the temperature of the ion source was 230 ℃.

2.6. Data processing

The data was processed using ChromaToF software (version 4.50.8.0), the signal-to-noise ratio was set at 100. Where analytical standards were not available in the laboratory peaks were annotated by comparison of experimental mass spectra with reference spectra of the National Institute of Standards and Technology (NIST14) library, with a minimum similarity threshold for a match set at 75 %; and as well as by

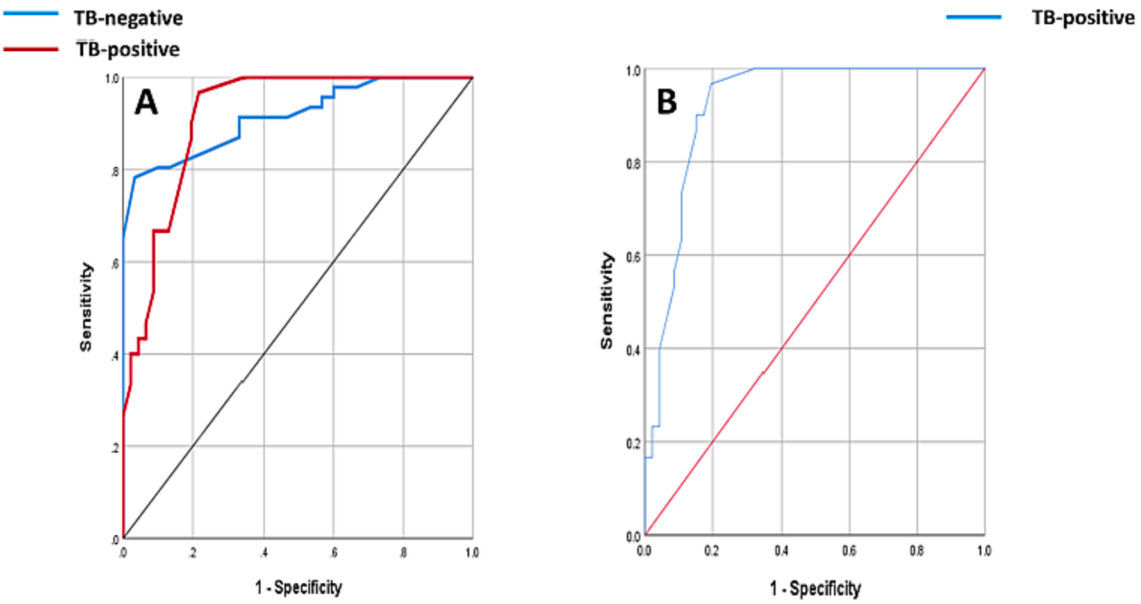

Fig. 3. The receiver operating characteristic (ROC) curves of the predictive modelling techniques based on the Fisher exact test-selected features (known TB-associated compounds from other bio-fluids): heptanal; octanal; 1-octene; heptane-3-ethyl-2-methyl; acetaldehyde and 1H-indene, 2,3 dihydro-1,1,3-trimethyl-3-phenyl-: (A) Artificial neural network in the multi-layered perceptron (ANN) with a sensitivity of 1.00 and a specificity of 0.94. The black diagonal line is a reference with an AUC of 0.5 (i.e. no predictive power) while the blue and red lines represent control and patient groups respectively. (B) Binary logistic regression (BLR) with a sensitivity of 0.87 and a specificity of 0.85. The red diagonal line is a reference with an AUC of 0.5 (threshold value), and the blue line represents the patient group. Both models had an area under the curve (AUC) of 0.92. (For interpretation of the references to colour in this figure legend, the reader is referred to the web version of this article.)

comparing experimental linear retention indices (LRIs) to literature LRIs to increase the level of confidence of peak annotation (Table 1). Compounds having a match of within ± 30 RI units are reported. LRIs were calculated from a C_8-C_{28} *n*-alkanes standard (Sigma-Aldrich, South Africa) according to the Van den Dool and Kratz method [28]. Artifacts (siloxanes) originating from the PDMS sampler (laboratory blank sampling bands) were removed before further data analysis (Fig. 2).

2.7. Statistical analysis

All calculations were carried out using SPSS® 25 statistical software (IBM® Corp. Armonk, New York, USA) except for the high performance variable selection (HPVS) calculation which was done using SAS 9.4 (Cary, North Carolina, USA). The relative abundance of peak areas across chromatograms was normalized using total useful peak area (TUPA). A schematic of the data processing workflow is depicted in Fig. 2.

2.7.1. Targeted analysis: Comparison to known TB-associated compounds from other biofluids

The Fisher's exact test was applied to a data set generated by means of an absent/present criterion to determine whether or not a compound was detected in a particular sample of a particular group to investigate significant differences of compounds between TB-positive and TB-negative states. Two predictive modelling techniques; artificial neural network multi-layered perceptron (ANN) and binary logistic regression (BLR), were applied and compared to determine the diagnostic power of the compounds and the most discriminatory compounds (Fig. 2).

2.7.2. Untargeted analysis: Exploring previously unreported compounds that might serve as diagnostic biomarkers

P-values were calculated using the Fisher's exact test done on all detected compounds (post siloxanes clean-up) based on an absent/present criterion to investigate significant differences of compounds between TB-positive and TB-negative states. HPVS calculations were performed on all detected compounds (normalized data) to minimize the size of the data without compromising the information. Principal component analysis (PCA) using the correlation matrix of compounds based on absent/present criterion or normalized peak areas was conducted to investigate clustering patterns between TB-positive and TB-negative states. ANN was applied to determine the diagnostic power of the compounds based on HPVS. A schematic diagram of the data processing workflow is depicted in Fig. 2.

3. Results and discussion

The study cohort consisted of 38 participants sampled during 2018, two PDMS sampler bands from each participant were analysed (m = 76 samples). The cohort comprised of two categories: patients (TB-positive) and controls (TB-negative, healthy). The use of Mylar® and Micropore tape excluded background compounds during sampling. Skin VOCs collection offers a relatively non-infectious matrix compared to exhaled breath, especially for airborne infections. Employing the skin VOC silicone rubber band sampler does not require skilled healthcare workers, it is portable and wearable, and its application is not cumbersome for either researcher or patient. Moreover, it does not interfere with medical procedures or hospital protocols. The nonpolar nature of PDMS was addressed by modifying the silicone rubber band with a polar solvent (ethanol) which increased the accumulation of polar compounds, and it served as a "keeper" [29]. GCxGC-TOFMS addressed the limitations of traditional GC–MS in that it ensured the separation and detection of complex chemical profiles. After removal of siloxane artifacts (originating from the PDMS samplers) from the data set 1500 compounds were retained. A targeted analysis was done where skin VOCs detected in this study were compared to known TB-associated compounds from other biofluids. Secondly, an untargeted analysis was done to find potential biomarkers previously unreported. Sensitivity and specificity as diagnostic markers were evaluated in comparison to existing diagnostic methods.

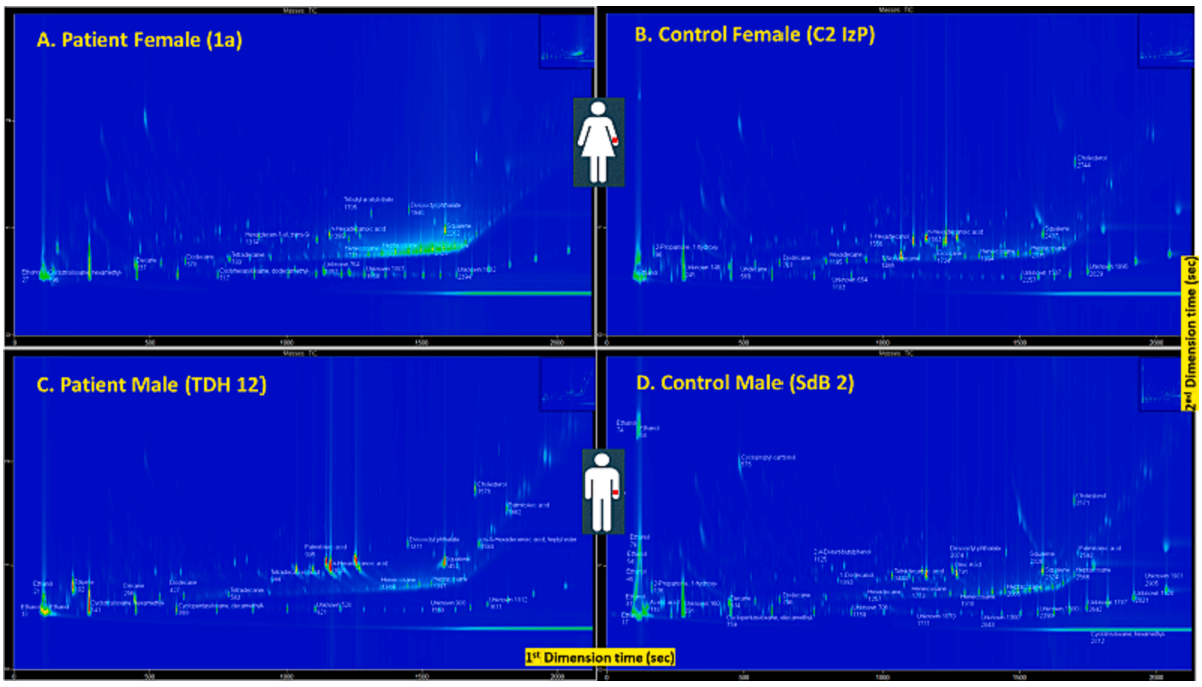

Fig. 4. Contour plots (TICs) of (A) Female TB-positive; (B) Female TB-negative; (C) Male TB-positive; D. Male TB-negative.

3.1. Targeted analysis: Comparison to known TB-associated compounds from other biofluids

In this study 27 compounds detected from the TB-positive participants' skin emanations (Table 1) were compounds associated with *M.tb*, as reported in the literature from the breath of confirmed active pulmonary TB patients and suspected TB patients, urine and sputum culture from TB patients, and *M.tb* cultures from *M.tb* colonies [13,14,30–32]. The compound classification was distributed as follows: alkanes (41 %), alkenes (11 %), alcohols (7 %), aldehydes (15 %), carboxylic acids (4 %), ketones (7 %), and aromatics (15 %) (Table 1).

Skin as a diagnostic matrix is indeed feasible, since compounds detected from TB-positive patient skin emanations matched those compounds found in other biofluids from active pulmonary TB patients. The Fisher's exact test (LOC 95 %) was used to test for significant differences between the TB-positive patients and the TB-negative healthy controls. Six compounds from the list of 27 targeted compounds known to be associated with TB, viz.: heptanal; octanal; 1-octene; heptane-3-ethyl-2-methyl; acetaldehyde and 1H-indene, 2,3 dihydro-1,1,3-trimethyl-3-phenyl- had p-values ≤ 0.05; and thus, there is a significant difference between the two groups for this set of potential biomarker compounds (Table 1). In terms of normalized peak areas 1-octene and heptane-3-ethyl-2-methyl were increased in the TB-positive group, while heptanal; octanal; acetaldehyde and 1H-indene, 2,3 dihydro-1,1,3-trimethyl-3-phenyl- were decreased in this group. Vishinkin et al. (2021) reported higher levels of acetic acid, 2-ethyl-1-hexanol, hexyl butyrate and toluene sampled from skin emanations from pulmonary active TB patients compared to non-TB patients and healthy controls [22]. However, in our study these compounds were found to be not significantly different between TB-positive and TB-negative individuals.

3.1.1. Predictive modelling

Two supervised machine learning (ML) techniques were used, the artificial neural network in the multi-layered perceptron (ANN) and binary logistic regression (BLR). In the ANN the data was split into a training set of 61.8 % (47 samples) and a test set of 38.2 (29 samples), the area under the receiver operating characteristic curve (AUROC) was 92 % with a sensitivity of 100 % and a specificity of 94 % (Fig. 3 A). This algorithm identified the putative compounds 1H-indene, 2,3 dihydro-1,1,3-trimethyl-3-phenyl; and heptane-3-ethyl-2-methyl as the most discriminatory, and allocated these with a normalized importance above 75 %. The BLR data set was split into a training set of 60.5 % (46 samples) and a validation set of 39.5 % (30 samples) and had a sensitivity of 87 % and a specificity of 85 %, with an AUROC of 92 % (Fig. 3 B). This model identified three compounds as the most discriminatory: 1H-indene, 2,3 dihydro-1,1,3-trimethyl-3-phenyl; heptane-3-ethyl-2-methyl; and acetaldehyde (normalized importance *p*-values ≤ 0.05).

Representative contour plots (TICs) of TB-positive, TB-negative, female and male participants are shown in Fig. 4. Marked differences in the chemical profiles are observed between TB-positive and TB-negative individuals, and between female and male individuals. Female patients, in general, exhibited an enriched complex mixture consisting predominantly of sterols, fatty acids and hydrocarbons [29] in the ^{1}D 1200 – 1700 s region of the chromatograms, corresponding to LRIs of 1800 to 2700. Abnormalities of lipid metabolism in a TB group characterized by an altered fatty acid metabolism was reported by Han et al. 2021 [33]. There are gender differences in lipid profiles, and the authors reported that "it has been demonstrated that the lipid status of the host is closely related to the pathogenesis of M. tuberculosis" [33].

3.2. Special participant categories: Extra-pulmonary TB and latent-TB

The patient group included an extra-pulmonary TB female patient and the control group included two latent-TB positive subjects (male and female). TB infection can occur in organs other than the lungs, this is termed extra-pulmonary TB. Latent-TB is defined as TB infection without clinical, bacteriologic or radiographic evidence of active TB. These two special classes were included to get a preliminary indication as to whether these would fall within the control or patient groups as per the original classification.

Fig. S1 (A-C) depicts contour plots of total ion chromatograms (TICs) of individuals within each special category (i.e. extra-pulmonary TB or latent-TB), and there are observable differences in the VOC profiles. The female extra-pulmonary TB patient (Fig. S1A) and the female latent-TB subject (Fig. S1B) have four compounds in common: n-hexadecanoic

Table 2
Compounds from extra-pulmonary TB-positive female, latent-TB positive female and male.

Classification	Compound	Biological matrix (literature)	Molecular weight	Molecular formula	CAS number	Retention Indices [1]DExperimental	Retention Indices Literature non-polar[#]	Extra-pulmonary TB female	Latent-TB positive female	Latent-TB positive male
Alkane	Pentane, 2,3-dimethyl-	Breath [13]	100	C7H16	565–59-3	<800	589		✓	
	Heptacosane	HMDB *Matrix unspecified	380	C27H56	593–49-7	2707	2705			✓
Alkene	1-Docosene	Plasma [34]	308	C22H44	1599–67-3	2193	2198			✓
Alcohol	Hexadecen-1-ol, *trans*-9-	N/A	240	C16H32O	64437–47-4	1869	1862	✓	✓	✓
	1-Eicosanol	Skin tissue [35]	298	C20H42O	629–96-9	2250	2254	✓		
Carboxylic acid	n-Decanoic acid	Blood, sweat*	172	C10H20O2	334–48-5	1371	1372			✓
	Dodecanoic acid	Blood*	200	C12H24O2	143–07-7	1571	1570			✓
	Z-7-Tetradecenoic acid	HMBD *Matrix unspecified	226	C14H26O2	0–00-0	1771	1777			✓
	Dodecanoic acid, 1-methylethyl ester	N/A	242	C15H30O2	10233–13-3	1620	1615			✓
	Hexadecenoic acid, Z-11-	N/A	254	C16H30O2	2416–20-8	1970	1976			✓
	n-Hexadecanoic acid	Blood*	256	C16H32O2	57–10-3	1966	1968	✓	✓	✓
	trans-13-Octadecenoic acid	Serum [36]	282	C18H34O2	693–71-0	2169	2175			✓
	Oleic Acid	Blood, saliva, urine *	282	C18H34O2	112–80-1	2170	2175		✓	
	cis-Vaccenic acid	Faeces*	282	C18H34O2	506–17-2	2173	2175	✓		
	Octadecanoic acid	Blood*	284	C18H36O2	57–11-4	2160	2167	✓	✓	✓
	1,3-Benzenedicarboxylic acid, bis(2-ethylhexyl) ester	N/A	390	C24H38O4	137–89-3	2719	2704			✓
Ketones	5,9-Undecadien-2-one, 6,10-dimethyl-, (E)-	Urine [37]	194	C13H22O	3796–70-1	1428	1420			✓
	7-Acetyl-6-ethyl-1,1,4,4-tetramethyltetralin	Sweat [38]	258	C18H26O	88–29-9	1994	1997	✓		
	Oxacyclotetradecane-2,11-dione, 13-methyl-	N/A	240	C14H24O3	74685–36-2	2136	2137			✓
Ester	Isopropyl palmitate	Saliva, urine*	298	C19H38O2	142–91-6	2015	2013	✓	✓	
Aromatic	2,4-Di-*tert*-butylphenol	Urine*	206	C14H22O	96–76-4	1759	1754			✓

N/A: not available.
< 800: Retention Index standard C_8-C_{28}.
* HMDB: Human Metabolome Database.
# Literature Retention Indices from NIST 14 library.

acid; hexadecen-1-ol, *trans*-9; isopropyl palmitate and octadecanoic acid. The female extra-pulmonary TB patient had two unique compounds: 7-acetyl-6-ethyl-1,1,4,4-tetramethyltetralin and 1-eicosanol, while the female latent-TB individual has two unique compounds: pentane-2,3-dimethyl and oleic acid. The male latent-TB individual (Fig. S1C) has three compounds in common with both female participants: n-hexadecanoic acid; hexadecen-1-ol-*trans*-9 and octadecanoic acid; while 12 compounds are unique to the male subject: 1) 5,9-undecadien-2-one,6,10-dimethyl-(E)-; 2) 2,4-di-*tert*-butylphenol; 3) dodecanoic acid; 4) dodecanoic acid,1-methylethyl ester; 5) Z-7-tetradecanoic acid; 6) n-decanoic acid; 7) unknown; 8) 1-docosene; 9) heptacosane; 10) *trans*-13-octadecanoic acid; 11) hexadecanoic acid, Z -cyclohexyl ester; 12) 1,3-benzenedicarboxylic acid, bis (2-ethylhexyl)ester and 14) oxacyclotetradecene-2,11-dione-13-methyl. The compounds with their respective experimental and literature LRIs are listed in Table 2. These special categories are further discussed in the following sections.

3.3. Untargeted analysis: Exploring potential TB-associated compounds previously unreported

The untargeted analysis provided the opportunity to explore skin VOCs associated with TB not previously reported in the literature. The Fisher's exact test was conducted on 1500 compounds using an absent/present criterion applied across the two groups (to establish whether a particular compound was more associated with any one of the two groups) to determine compounds that had a significant difference between TB-positive and TB-negative states. Three hundred and twenty-six (326) compounds with a p-value ≤ 0.05 were retained [29]. Principal component analysis (PCA) was conducted using the 326 compounds based on both absent/present criterion, and as well as on normalized peak areas to investigate whether discrimination between patients and controls would emerge in both approaches (Fig. 5 A and B). The PCA plots show distinct grouping between the two classes (except for a single patient outlier). This clustering is an indication that the compounds can discriminate between the two groups, and thus have the prospect of being used as diagnostic biomarkers. Interesting observations were that the extra-pulmonary TB female participant featured within the patient

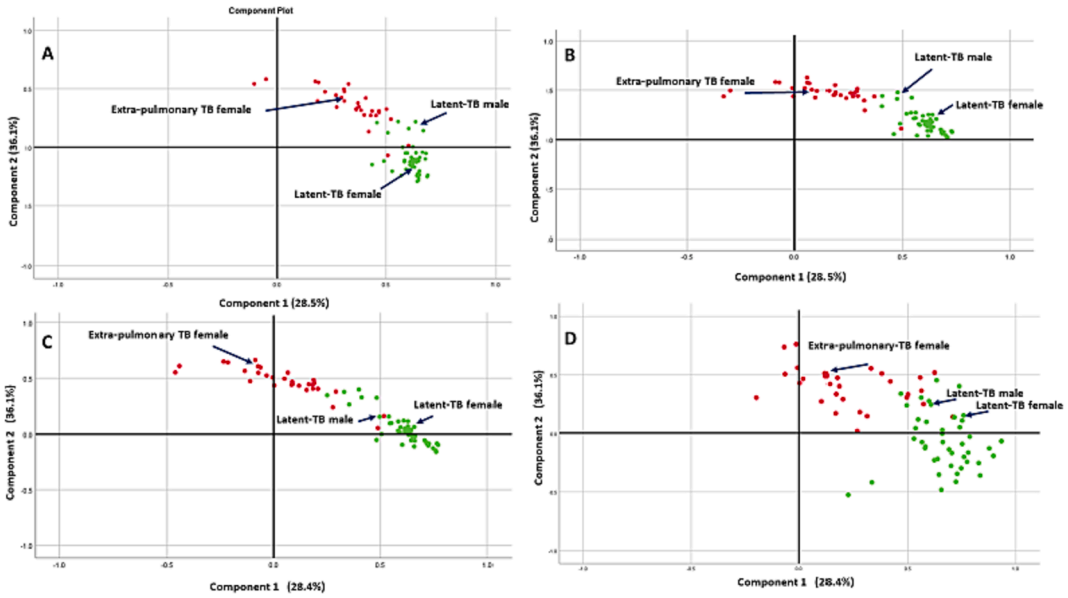

Fig. 5. (Top) Untargeted: principal component analysis (PCA) plots generated using the 326 compounds with a p-value ≤ 0.05 (Fisher exact test). Plot A was created using the absent or present criteria, and plot B using normalized peak areas. The red dots represent patients, while the green dots represent controls. (Bottom) Untargeted: PCA plots generated of patients *versus* controls using the 16 high performance variable selection (HPVS) compounds. Plot C is based on the absent or present criteria and plot D is based on normalized peak areas. Red dots represent patients and the green dots are the controls. (For interpretation of the references to colour in this figure legend, the reader is referred to the web version of this article.)

Table 3
Compounds selected by the high performance variable selection (HPVS) analysis.

Compound	Molecular weight	Molecular formula	CAS number	RI experimental 1D non-polar	RI Literature[#]	Importance	Normalised importance	*p*-value
Hexane, 3-methyl-	100	C7H16	589–34-4	<800	653	0.109	100 %	0
2-Octylcyclopropene-1-heptanol	266	C18H34O	54467–85-5	2049	2056	0.099	91 %	0.008
Pyrene, hexadecahydro-	218	C16H26	2435–85-0	1526	1502	0.073	67 %	0.032
Celestolide	244	C17H24O	13171–00-1	1856	1857	0.068	62 %	0.008
1,4-Methanobenzocyclodecene, 1,2,3,4,4a,5,8,9,12,12a-decahydro-	202	C15H22	74708–73-9	1583	1567	0.062	57 %	0.028
2-Tridecene, (E)-	182	C13H26	41446–58-6	1348	1321	0.055	51 %	0
Cyclopentaneacetic acid, 3-oxo-2-pentyl-, methyl ester	226	C13H22O3	24851–98-7	1675	1657	0.052	47 %	0
2-Decenal, (Z)-	154	C10H18O	2497–25-8	1242	1212	0.048	44 %	0.036
Maltol	126	C6H6O3	118–71-8	1077	1063	0.047	43 %	0
2(3H)-Furanone, 5-methyl-	98	C5H6O2	591–12-8	902	897	0.044	40 %	0.001
Bicyclo[4.1.0]heptane, 3,7,7-trimethyl-, [1S-(1α,3α,6α)]-	138	C10H18	18968–23-5			0.044	40 %	
1-Heptene	98	C7H14	592–76-7	<800	707	0.04	37 %	0.027
Ethanol, 2-(2-ethoxyethoxy)-	134	C6H14O3	111–90-0	997	1012	0.032	29 %	0.002
Nonane, 2-methyl-	142	C10H22	871–83-0	951	951	0.029	26 %	0.036
Benzoic acid	184	C11H20O2	2499–59-4	1255	1272	0.026	24 %	0.002
2-Propenoic acid, ethenyl ester	98	C5H6O2	2177–18-6	<800	666	0.026	24 %	1

<800: Retention Index standard C_8-C_{28}.
[#] Literature Retention Indices from NIST 14 library.

group, and the latent-TB individuals featured close to or within the control group in both PCA approaches (Fig. 5 A and B). These special category participant observations suggest that skin VOCs can be used to discriminate between controls (including latent-TB) and extra-pulmonary TB states, however, a larger sample size is required to confirm this.

3.3.1. *High performance variable selection*

High performance variable selection (HPVS) was conducted on the total number of compounds detected in this study (1500), to investigate whether reducing the number of VOCs to a smaller size was feasible, which would be more practical for a clinical test. In a bid to reduce the number of compounds in the data set without compromising the original information, all compounds were included in the HPVS software calculation regardless of the p-value. The HPVS returned 16 compounds (Table 3).

Table 3 provides the weights or importance of each compound in the artificial neural network in the multi-layered perceptron model. 3-methylhexane and 2-octylcyclopropene-1-heptanol have the highest importance, with respective normalised importance of 100 % and 91.00 %. This means these two compounds had the most contribution to the model, suggesting that these are good candidates for use as diagnostic

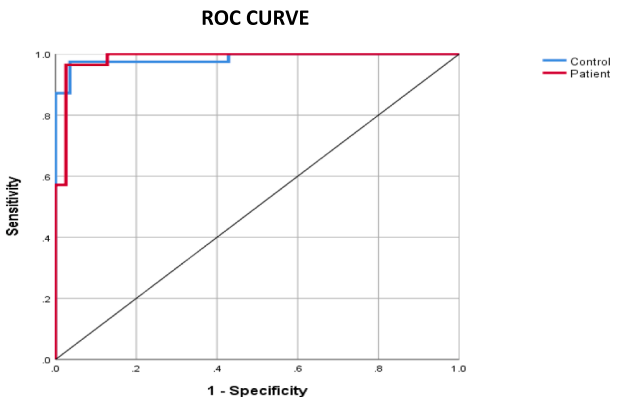

Fig. 6. ROC curve evaluating the accuracy of the skin VOC test based on the 16 HPVS-selected features (nonane-2-methyl-; 3-methylhexane; 1-heptene; 2-tridecene,(E)-; 2-octylcyclopropene-1-heptanol; maltol; ethanol-2-(2-ethoxy)-; 2-decenal,(Z)-; celestolide; bicyclo[4.1.0]heptane,3,7,7-trimethyl-[1S-1α,3α,6α]-; pyrene, hexadecahydro-; 1.4-methanobenzocyclodecene, 1.2.3.4.4a.5.8.9.12.12a-decahydro-; cyclopentaneacetic acid,3-oxo-2-pentyl-, methyl ester; 2-propenoic acid, ethenyl ester; benzoic acid and 2(3H)-furanone, 5-methyl- obtained using artificial neural network in the multi-layered perceptron (ANN) mode predictive modelling technique. The black diagonal line is a reference with an AUC of 0.5 which is the threshold value, while the blue and red lines represent control and patient groups respectively. The testing set and hold-out set had sensitivities and specificities of 83 %, 88 %, and 100 %, 86 % respectively. The ROC curve has an AUC of 99 % which indicates the model has an excellent classification rate. Training set = 62 % (n = 47 samples), testing set = 26 % (n = 20 samples) and hold-out set = 12 % (n = 9 samples). (For interpretation of the references to colour in this figure legend, the reader is referred to the web version of this article.)

biomarkers for TB. Another point to note is that these compounds with a high importance have p-values below 0.05 (Table 3). The following compounds had the least importance which was below 30 %: ethanol, 2-(2-ethoxyethoxy)-; nonane, 2-methyl-; benzoic acid; and 2-propenoic acid, ethenyl ester. 2-Propenoic acid, ethenyl ester has a p-value of one, and therefore its place among the least important compounds is not surprising, but rather confirmation of the suitability of the Fisher exact test, and the decision to focus on compounds with a p-value $\leq$ 0.05.

PCA was then done using the 16 HPVS-selected compounds based on two approaches, i.e., absent/present criterion and normalized peak areas. Fig. 5C and D depicts both PCA plots, which show two distinct groups of patients and controls for both approaches, indicating that the 16 compounds can discriminate between TB-positive and TB-negative states. As before, the female extra-pulmonary female participant samples were within the patient group, while the latent TB subjects were close to, or within the control group (Fig. 5C.). Where the latent TB female subject clustered within the control group in the PCA based on the absent/present criterion, here the participant samples featured just outside of the control cluster of the PCA (Fig. 5D).

The discriminatory precision of the 16 HPVS compounds was investigated by predictive modelling using the artificial neural network multi-layered perceptron technique, the receiver operating characteristic (ROC) curve is provided in Fig. 6. The data was split into a training set with 62 % (n = 47 samples), testing set with 26 % (n = 20 samples) and the hold-out set with 12 % (n = 9 samples). The training set is used to train the model, the testing set evaluated the trained model and the hold-out set validated the accuracy of the model. The testing set and hold-out set had sensitivities and specificities of 83 %, 88 %, and 100 %, 86 % respectively and an area under the curve (AUC) of 0.99. Results compare favourably to that of Saktiawati et al. (2019) and Sekyere et al. (2019) which report sensitivities and specificities of 93 % and 93 % (electronic nose), 82 % and 92 % (breath), and 79.6 % and 90.3 % (GeneXpert) [39,40].

The model reported two compounds, 3-methylhexane and 2-octylcyclopropene-1-heptanol, to have a normalised importance above 75 %. Normalized peak areas were increased in the TB-positive group. Investigation into these two compounds revealed that 3-methylhexane is listed as a secondary metabolite detected in blood on the Human Metabolome Database (HMDB) and it was not found in the Kyoto Encyclopedia of Genes and Genomes (KEGG) compound database. 2-Octylcyclopropene-1-heptanol is listed as a chemical component of at least three medicinal plants; *Gloriosa superba* flower, *Alysicarpus glumaceus* and *Artemisia herba* and as a bioactive compound in *Solanum Xanthocarpum* [41–44]. Therefore, it should be considered that the presence of 2-octylcyclopropene-1-heptanol may point to patients self-medicating with herbal remedies. However, this needs to be investigated.

4. Conclusion

Through an analysis of skin volatile organic compounds (VOCs), we confirm 27 compounds already known to be associated with TB from other biofluids, and report 16 new compounds of diagnostic importance. The sensitivity and specificity of the non-invasive skin test showed favourable performance compared to other diagnostic methods such as electronic nose, breath analysis, and GeneXpert. We have demonstrated that skin VOCs can differentiate between TB-positive and TB-negative individuals. As such, the skin VOC test is a promising tool for diagnostic applications and warrants further investigation involving a larger study cohort, and confirmation of biomarker identity using high resolution mass spectrometry or expansion of the number of analytical standards used.

Declaration of Competing Interest

The authors declare that they have no known competing financial interests or personal relationships that could have appeared to influence the work reported in this paper.

Data availability

Data will be made available on request.

Acknowledgments

The authors gratefully acknowledge the late Prof Anton Stoltz (†2020), Department of Internal Medicine, Division of Infectious Diseases, University of Pretoria, for access to patients and funding, we thank Dr Katherine Anderson for phlebotomy services, Ms Tebogo Magongoa for assistance with the hospital administration, Ms Marizane du Pisanie for the NHLS labtrek services, Ms Tanita Cronjé for discussion regarding statistical analysis, and Mr Daniel Pretorius for assisting with analyses of analytical standards and selected samples for analyte confirmation.

Appendix A. Supplementary material

Supplementary data to this article can be found online at https://doi.org/10.1016/j.jchromb.2023.123937.

References

[1] S.D. Lawn, A.I. Zumala, Tuberculosis, Lancet. 378 (9785) (2011) 57–72.
[2] M. Gengenbacher, S.H.E. Kaufmann, Mycobacterium tuberculosis: success through dormancy, FEMS Microbiol. Rev. 36 (3) (2012) 514–532.
[3] L.M. Parsons, C. Gutierrez, E. Lee, C.N. Paramasivan, A. Abimiku, S. Spector, G. Roscigno, J. Nkengasong, Laboratory diagnosis of tuberculosis in resource-poor countries: challenges and opportunities, Clin. Microbiol. Rev. 24 (2) (2011) 314–350.
[4] A.M. Elliott, K. Namaambof, Negative sputum smear results in hiv-positive patients with pulmonary tuberculosis in Lusaka Zambia, Tuber Lung Dis. 74 (3) (1993) 191–194.

[5] G.G.L. Avalos, E.P.M. de Oca, Classic and new diagnostic approaches to childhood tuberculosis, J. Trop. Med. 818219 (2012).
[6] J. Dinnes, J. Deeks, H. Kunst, A. Gibson, E. Cummins, N. Waugh, F. Drobniewski, A. Lalvani, A systematic review of rapid diagnostic tests for the detection of tuberculosis infection, Health Technol. Assess. 11 (3) (2007) 1–196.
[7] M. Beccaria, C. Bobak, B. Maitshotlo, T.R. Mellors, G. Purcaro, F. Franchina, C.A. Rees, M. Nasir, A. Black, J.E. Hill, Exhaled human breath analysis in active pulmonary tuberculosis diagnostics by comprehensive gas chromatography-mass spectrometry and chemometric techniques, J.Breath Res. 5 (13) (2019) 016005. Available from: http://doi.org/10.1088/1752-7163/aae80e.
[8] D. Beukes, M. van Reenen, L. Du Toit, I. du Preez, Tuberculosis is associated with sputum metabolome variations, irrespective of patient sex or HIV status: an untargeted GCxGC-TOFMS study 2023, Metabolomics. 19 (6) (2023) 55. Available from: https://doi.org/10.1007/s11306-023-02017-7.
[9] J. Eshima, S. Ong, T.J. Davis, C. Miranda, D. Krishnamurthy, A. Nachtsheim, J. Stufken, C. Plaisier, J. Fricks, H.D. Bean, B.S. Smith, Monitoring changes in the healthy female metabolome across the menstrual cycle using GC×GC-TOFMS, J. Chromatogr. B 1121 (2019) 48–57.
[10] K. Dheda, M. Ruhwald, G. Theron, J. Peter, W.C. Yam, Point-of-care diagnosis of tuberculosis: past, present and future, Respirology. 18 (2) (2013) 217–232.
[11] S.T. Chambers, The scent of mycobacterium tuberculosis, Tuberculosis. 88 (2008) 317–323.
[12] M. Phillips, Method for the collection and assay of volatile organic compounds in breath, Anal. Biochem. 247 (1997) 272–278.
[13] A.H.J. Kolk, J.J.B.N. Van Berkel, M.M. Claassens, E. Walters, S. Kuijper, J. W. Dallinga, F.J. Van Schooten, Breath analysis as a potential diagnostic tool for tuberculosis, Int. J. Tuberc. Lung Dis. 16 (6) (2012) 777–782.
[14] M. Phillips, R.N. Cataneo, R. Condos, G.A. Ring, J. Greenberg, V. La, M.I. Munawar, O. Tietje, Volatile biomarkers of pulmonary tuberculosis in the breath, Tuberculosis. 87 (2007) 44–52.
[15] S. Sethi, R. Nanda, T. Chakraborty, Clinical application of volatile organic compound analysis for detecting infectious diseases, Clin. Microbiol. Rev. 26 (3) (2013) 462–475.
[16] N.A. Dang, H.G. Janssen, A.H.J. Kolk, Rapid diagnosis of TB using GC–MS and chemometrics, Bioanalysis. 5 (24) (2013) 3079–3097.
[17] S.D. Lawn, Point-of-care detection of lipoarabinomannan (lam) in urine for diagnosis of hiv-associated tuberculosis: a state of the art review, BMC Infect. Dis. 12 (103) (2012) 1–20.
[18] J. Minion, E. Leung, E. Talbot, K. Dheda, M. Pai, D. Menzies, Diagnosing tuberculosis with urine lipoarabinomannan: systematic review and meta-analysis, Eur. Respir. J. 38 (6) (2011) 1398–1405.
[19] F. Buljubasic, G. Buchbauer, The scent of human diseases: A review on specific volatile organic compounds as diagnostic biomarkers, Flavour Fragr. J. 30 (1) (2015) 5–25.
[20] C. Turner, B. Parekh, C. Walton, P. Španěl, D. Smith, M. Evans, An exploratory comparative study of volatile compounds in exhaled breath and emitted by skin using selected ion flow tube mass spectrometry, Rapid Commun. Mass Spectrom. 22 (4) (2008) 526–532.
[21] J.A. Pickett, R.C. Smallegange, T. Bousema, J.G. Logan, A.O. Busula, M.A. Voets, A. Robinson, J.C. Caulfield, R.W. Sauerwein, N.O. Verhulst, K.B. Beshir, C. J. Sutherland, J.G. de Boer, M.A. Birkett, S.J. Powers, P. Winskill, J. Muwanguzi, D. K. Masiga, W. Takken, W.R. Mukabana, Plasmodium associated changes in human odour attract mosquitoes, Proc. Natl. Acad. Sci. 115 (18) (2018) 201721610.
[22] R. Vishinkin, R. Busool, E. Mansour, F. Fish, A. Esmail, P. Kumar, A. Gharaa, J. C. Cancilla, J.S. Torrecilla, G. Skenders, M. Leja, K. Dheda, S. Singh, H. Haick, Profiles of volatile biomarkers detect Tuberculosis from Skin, Adv. Sci. 8 (2021) 2100235, https://doi.org/10.1002/advs.202100235 Advanced Science.
[23] A.P. Roodt, Y. Naudé, E. Rohwer, Human skin volatiles: Passive sampling and GC×GC-ToFMS analysis as a tool to investigate the skin microbiome and interactions with anthropophilic mosquito disease vectors, J. Chromatogr. B 1097–1098 (2018) 83–93.
[24] M. Wooding, E. Rohwer, Y. Naudé, Chemical profiling of the human skin surface for malaria vector control via a non-invasive sorptive sampler with GC× GCTOFMS, Anal. Bioanal. Chem. 412 (23) (2020) 5759–5777.
[25] M. Wooding, E.R. Rohwer, Y. Naudé, Non-invasive sorptive extraction for the separation of human skin surface chemicals using comprehensive gas chromatography coupled to time-of-flight mass spectrometry: A mosquito-host biting site investigation, J. Separ. Sci. 43 (22) (2020) 4202–4215.
[26] Y. Naudé, P. Gorst-Allman, E. Rohwer, A cheap and simple passive sampler using silicone rubber for the analysis of surface water by gas chromatography–time of flight mass spectrometry, Water SA. 41 (2) (2015) 182–188.
[27] S. Triñanes, M.T. Pena, M.C. Casais, M.C. Mejuto, Development of a new sorptive extraction method based on simultaneous direct and headspace sampling modes for the screening of polycyclic aromatic hydrocarbons in water samples, Talanta. 132 (2015) 433–442.
[28] H. Van den Dool, P.D. Kratz, A generalization of the retention index system including linear temperature programmed gas-liquid partition chromatography, J Chromatogr a. 11 (1963) 463–471.
[29] P.C.K. Makhubela, A non-invasive human skin sampling technique for the detection of volatile organic compounds associated with *Mycobacterium tuberculosis*. MSc dissertation 2022. www.up.ac.za. Under embargo until June 2024.
[30] K.M. Banday, K.K. Pasikanti, E.C.Y. Chan, R. Singla, K.V.S. Rao, V.S. Chauhan, R. K. Nanda, Use of urine volatile organic compounds to discriminate tuberculosis patients from healthy subjects, Anal Chem. 83 (2011) 5526–5534.
[31] R. Pal, S. Dahal, A. Gurung, Exhaled breath analysis in tuberculosis case detection: the new horizon, Nepal J Epidemiology. 3 (2) (2013) 243–244.
[32] M. Phillips, V. Basa-Dalay, G. Bothamley, R.N. Cataneo, P.K. Lam, M.P. R. Natividad, P. Schmitt, J. Wai, Breath biomarkers of active pulmonary tuberculosis, Tuberculosis. 90 (2) (2010) 145–151.
[33] Y.-S. Han, J.-X. Chen, Z.-B. Li, J. Chen, W.-J. Yi, H. Huang, L.-L. Wei, T.-T. Jiang, J.-C. Li, Identification of potential lipid biomarkers for active pulmonary tuberculosis using ultra-high-performance liquid chromatography-tandem mass spectrometry, EBM 246 (2021) 387–399.
[34] H. Zhao, C. Wang, N. Zhao, W. Li, Z. Yang, X. Liu, W. Le, X. Zhang, Potential biomarkers of Parkinson's disease revealed by plasma metabolic profiling, J. Chromatogr. b. 1081–1082 (2018) 101–108.
[35] T. Abaffy, M. Möller, D.D. Riemer, C. Milikowski, R.A. Defazio, A case report – volatile metabolic signature of malignant melanoma using matching skin as a control, J. Cancer Sci Ther. 3 (6) (2011) 140–144.
[36] D. Wang, X. Wang, J. Kong, J. Wu, M. Lai, GC-MS-based metabolomics discovers a shared serum metabolic characteristic among three types of epileptic seizures, Epilepsy Res. 126 (2016) 83–89.
[37] T. Ligor, P. Adamczyk, T. Kowalkowski, I.A. Ratiu, A. Wenda-Presile, B. Buszewski, Analysis of VOCs in urine samples directed towards of bladder cancer detection, Mol. 27 (2022) 5023.
[38] M.-J. Choi, C.-H. Oh, 2nd dimensional GC-MS analysis of sweat volatile organic compounds prepared by solid phase micro-extraction, Technol Health Care. 22 (2014) 481–488.
[39] A.M.I. Saktiawati, D.D. Putera, A. Setyawan, Y. Mahendradhata, T.S. van der Werf, Diagnosis of tuberculosis through breath test: A systematic review, EBioMedicine. 46 (2019) 202–214.
[40] J.O. Sekyere, N. Maphalala, L.A. Malinga, N.M. Mbelle, N.E. Maningi, A comparative evaluation of the new genexpert mtb/rif ultra and other rapid diagnostic assays for detecting tuberculosis in pulmonary and extra pulmonary specimens, Sci Rep. 12 (9) (2019) 16587.
[41] M. Nithya, C. Ragavendian, D. Natarajan, Antibacterial and free radical scavenging activity of a medicinal plant Solanum Xanthocarpum, Int. J. Food Prop. 21 (1) (2018) 313–327.
[42] R. Kavitha, A.M. Uduman, Determination of phytochemicals in Gloriosa Superba flower extract using gas chromatography and mass spectroscopic technique, J. Pharmacogn. Phytochem. 7 (6) (2018) 349–352.
[43] A. Nezhadal, M. Akbarpour, S.B. Zarrabi, Chemical composition of the essential oil from the aerial parts of Artemisia Herba, E-J. Chem. 5 (3) (2008) 557–561.
[44] F. Khan, M.G. Magaji, I. Abdu-Aguye, I.M. Hussaini, A. Hamza, A.B. Olarukooba, M.A. Sani, I.M. Maje, Phytochemical profiling of the bioactive principles of Alysicarpus glumaceus (Vahl) DC. aerial parts, Istanbul J. Pharm. 51 (2) (2020) 228–238.